Title:

Impaired basal and running-induced hippocampal neurogenesis **coincides** with reduced Akt signaling in adult R6/1 HD mice.

Authors:

Mark I Ransome[1†] and Anthony J Hannan[1,2]

Affiliations:

1. The Florey Institute of Neuroscience and Mental Health, University of Melbourne, Parkville, Victoria, 3010, Australia.

2. Department of Anatomy and Cell Biology, The University of Melbourne, Parkville, Victoria, 3010., Australia.

Correspondence:

† Mark I Ransome

email: mark.ransome@florey.edu.au

ph: +61 3 90356533 fx: +61 3 9344 1707

Address: The Florey Institute of Neuroscience and Mental Health, Kenneth Myer Building, Melbourne University, Parkville, VIC., 3010., Australia.

Abbreviations:

AHN, adult hippocampal neurogenesis; BrdU, 5-bromodeoxyuridine; BS, blocking solution; DCX, doublecortin; DG, dentate gyrus; GFAP, glial fibrillary acid protein; GCL, granule cell layer; GH, growth hormone; HD, Huntington's disease; IGF-1, insulin-like growth factor-1; IP, intraperitoneal; mHtt, mutant Huntingtin protein; O/N, overnight; PB, phosphate buffer; PBS, phosphate-buffered saline; SGZ, sub-granular zone;

Abstract

Huntington's disease (HD) is a fatal neurodegenerative disorder affecting a range of cellular and molecular functions in the brain. Deficits in adult hippocampal neurogenesis (AHN) have been documented in the R6/1 mouse model of HD. Here we examined basal and running-induced neuronal precursor proliferation in adult female and male R6/1 HD mice. We further tested whether sequential delivery of voluntary running followed by environmental enrichment could synergistically enhance functional AHN in female R6/1 HD mice. R6/1 HD mice engaged in significantly reduced levels of voluntary running, with males showing a more severe deficit. Basal neural precursor proliferation in the hippocampal sub-granular zone remained unchanged between female and male R6/1 HD mice and neither sex significantly responded to running-induced proliferation. While discrete provision of running wheels and enriched environments doubled AHN in adult female R6/1 HD mice it did not reflect the significant 3-fold increase in female wildtypes. Nevertheless, triple-label c-Fos/BrdU/NeuN immunofluorescence and confocal microscopy provided evidence that the doubling of AHN in female R6/1 HD mice was functional. Intrinsic cellular dysfunction mediated by protein aggregates containing mutant huntingtin (mHtt) did not appear to coincide with AHN deficits. In the hippocampus of female R6/1 HD mice, proliferating precursors and 6 week old adult-generated neurons were devoid of mHtt immuno-reactive aggregates, as were endothelial, microglial and astroglial cells populating the neurogenic niche. Serum transforming growth factor-β concentrations remained unaltered in female R6/1 HD mice as did hippocampal levels of proliferating microglia and glial fibrillarly acidic protein expression. Examining the growth hormone/insulin-like growth factor 1 (GH/IGF-1) axis showed no change in base-line serum GH between genotypes. However, despite a reduced distance, acute running increases serum GH in both female wildtype and R6/1 HD mice. Serum IGF-1 levels were increased in female R6/1 HD mice compared to wildtypes during daytime inactive period, while hippocampal levels of the IGF-1 receptor remained unchanged. Running induced Akt phosphorylation in the hippocampus of female wildtype mice, which was not reflected in R6/1 HD mice. Total Akt levels were decreased in the hippocampus of both control and running R6/1 HD mice. **Our results show adult-generated hippocampal neurons in female R6/1 HD mice express c-Fos** and that running and Akt signaling deficits may mediate reduced basal and running-induced AHN levels.

Key words:

IGF-1; hippocampal neurogenesis; Huntington's disease; exercise; Akt; growth hormone, R6/1 transgenic mice.

Introduction

Huntington's disease (HD) is an autosomal dominantly inherited neurodegenerative disorder. The pathophysiology of HD manifests primarily in the brain with progressive symptomology that includes cognitive, psychiatric and motor dysfunction (Borrell-Pages et al. 2006; Cattaneo et al. 2005; HDCRG 1993; Reiner et al. 1988). The onset of HD typically occurs in the adult with a disease outcome that is invariably fatal. At the genetic level HD results from an expanded cytosine-adenine-guanine (CAG) trinucleotide repeat that encodes a poly-glutamine (polyQ) tract in the N-terminus of the huntingtin protein (Hatters 2008; HDCRG 1993). The expanded polyQ stretch imparts a propensity for the mutant Huntingtin protein (mHtt) to form intracellular aggregates and proteolytic cleavage allows mutant fragments to enter the nucleus and form protein aggregates (Wellington et al. 1998). The presence of polyQ-containing aggregates in the brain is a pathological hallmark of HD and is postulated to contribute to neuronal dysfunction and death (Davies et al. 1997). The R6/1 transgenic mouse line closely models human HD, including the development of aggregates, and provides an important platform to study underlying disease mechanisms and therapeutic strategies (Gil & Rego 2009).

Cell-based approaches remain a focus of therapeutic intervention for HD, which hitherto remains without effective therapeutic intervention (Clelland et al. 2008). However, cell-based therapy for HD has had equivocal outcomes and preclinical studies are paramount in developing effective neural regeneration approaches. The emergence of adult neurogenesis as an endogenous neuronal repair mechanism has provided therapeutic appeal to a variety of neurodegenerative disorders including HD (Vandenbosch et al. 2009). Adult neurogenesis ensues throughout the life of mammals in discreet niches, including the sub-granular zone (SGZ) of the hippocampus. Adult hippocampal neurogenesis (AHN) is postulated to be an important neuronal substrate mediating the positive effects of running and enrichment on learning and memory (Lafenetre et al. 2011). Deficits in AHN have been demonstrated in several rodent models of HD (Gil et al. 2004; Gil et al. 2005; Lazic et al. 2004; Simpson et al. 2011) and reviewed in; (Gil-Mohapel et al. 2011). AHN deficits in the R6/1 HD transgenic mouse model manifest progressively and could underlie the impaired cognitive and depressive-like behaviours that develop in this mouse model (Grote et al. 2005; Lazic et al. 2004; Lazic et al. 2006; Ransome et al. 2012).

A diversity of environmental, physiological and genetic factors contribute to the regulation of AHN levels. Exercise in the form of voluntary running stimulates neuronal

precursor proliferation to increase AHN levels and improve cognition (Ransome & Turnley 2008; van Praag et al. 1999b; van Praag et al. 1999a). R6/1 HD mice given access to voluntary running have sex-dependent responses to exercise-induce neurotrophin expression (Zajac et al. 2010). However, whether sex is a determinant of exercise-induced AHN in R6/1 HD mice remains unknown. Cognitive stimulation through environmental enrichment also increases AHN levels but does so by promoting neuronal survival (Kempermann et al. 1997). Although R6/1 HD mice remain responsive to environmental enrichment strategies aimed at improving AHN and cognition (Lazic et al. 2004; Lazic et al. 2006; Nithianantharajah et al. 2008; Pang et al. 2006), there remains a paucity of evidence demonstrating functional AHN. Our current study was performed to examine whether sex affects basal or running-induced AHN in R6/1 HD and wildtype mice and **determine whether adult-generated hippocampal neurons express c-Fos** in R6/1 HD mice.

Materials and Methods

Animals

Female and male R6/1 HD transgenic mice on the CBA/BL6 genetic background and CBA/BL6 wildtype littermates were obtained from stocks maintained at the Howard Florey Institute. Over-expression of exon 1 of the human *huntingtin* gene with approximately 125 CAG repeats driven by the human *huntingtin* promoter in R6/1 HD mice provides an accurate model of human adult-onset HD (Gil & Rego 2009; Mangiarini et al. 1996). Rear-paw clasping is a behavioral trait indicative of motor dysfunction in R6/1 HD mice (J. Y. Li et al. 2005) and was used to document motor competency in all R6/1 HD animals used in this study. Mice were given food and water *ad libitum* and kept on a constant 12-hour light /dark cycle. The use of experimental animals was approved by the Animal Ethics Committee of the Howard Florey Institute. All procedures using experimental animals were conducted in strict accordance with National Health & Medical Research Council of Australia guidelines and in a manner that minimized animal distress.

Peroxidase Immunohistochemistry

Peroxidase immunohistochemistry was performed as previously described (Ransome & Turnley 2007, 2008). Floating sections were washed in PBS and then incubated in 1% H_2O_2 in PBS for 30 minutes at 20^{O}C to block endogenous peroxidase activity. Sections were washed further in PBS and then for BrdU incubated in 1 M HCl for 30 minutes at 37^{O}C for antigen unmasking. Sections were then washed extensively in PBS and incubated in blocking solution (BS) consisting of 5% normal Donkey serum (Merck-Millipore, Kilsyth, Australia) and 0.2% Triton-X100 (Sigma-Aldrich, Castle Hill, Australia) in PBS for 1 hour at 20^{O}C. Sections were then incubated overnight (O/N) at 20^{O}C in the following primary antibodies diluted in BS; sheep anti-BrdU (1/500; Exalpha Biologicals, Shirley, USA), rabbit anti-Ki67 (1/200; Lab Vision Corporation, Thermo Fisher Scientific, Scoresby, Australia), rabbit anti-caspase-3 (1/200; Cell Signalling Technologies, Danvers, USA) or rabbit anti-Iba-1 (1/300; Wako Pure Chemicals, Osaka, Japan). Sections were washed in PBS before being incubated for 2 hours at 20^{O}C in respective secondary antibodies diluted 1/500 in BS; biotinylated goat anti-sheep or biotinylated goat anti-rabbit (both Vector Laboratories, Burlingame, USA). After further washes in PBS,

sections were incubated in VectaStain ABC solution (1:100, Vector Laboratories) for 45 minutes at 20^{O}C, washed again in PBS and then developed in diaminobenzidine (DAB) liquid chromogen kit (1:50, Dako, Botany, Australia). Sections were rinsed in PBS, mounted onto slides and after drying were lightly counterstained in hematoxylin and coverslipped with DPX (Sigma-Aldrich).

Peroxidase-labeled cell counts

Peroxidase immuno-labeled cells were quantitated in the SGZ, GCL and hilus as previously described (Ransome & Turnley 2007, 2008) using an Olympus BX61 microscope with an UPlan FL N 60x objective lens installed with an eye-piece 10x10 grid (Olympus, Mount Waverley, Australia). Slides were coded and cell counting was conducted with the observer blind to the identity of anatomically matched sections. The SGZ was defined as 16μm (approximating 2-cell widths) either side of the junction between the granule cell layer (GCL) and the hilus in adjacent series of 6 serial sections spaced 240μm apart corresponding to bregma – 1.34 mm to bregma – 2.54 mm (Paxinos & Franklin 2001). In each section digital images were captured using a 10x objective lens and a Q Imaging 5.0 color RTV digital camera (Olympus) and Image-Pro plus software (MediaCybernetics, Rockville, USA) to measure SGZ length and GCL and hilus area. SGZ length was multiplied by 32 (SGZ width) and 40 (section thickness), while GCL and hilus areas were multiplied by 40 (section thickness) to provide volumes in μm^3 that were then converted to mm^3. For each section the number of (+)cells was combined with the corresponding volume to yield a cell density. Results are expressed as the mean cell number per mm^3 ± sem.

Multi-label immunofluorescence immunohistochemistry

Doublecortin/BrdU: Floating sections were washed in PBS then incubated in BS for 1 hour at 20^{O}C, then in goat anti-doublecortin (DXC, C-18, 1/400, Santa Cruz Biotechnology, Santa Cruz, USA) in BS, O/N at 20^{O}C. Sections were then washed in PBS and incubated in CY3-conjugated donkey anti-goat (1/400, Jackson ImmunoResearch, West Grove, USA) in BS for 2 hours at 20^{O}C. Sections were checked for staining quality before proceeding with BrdU labeling by incubating sections in 2 M HCl at 37^{O}C for 30 minutes. After extensive washing in PBS sections were incubated in sheep anti-BrdU (1/500, Exalpha) in BS, O/N at 20^{O}C. Sections were washed and incubated in Alexa Fluor 488-conjugated donkey anti-sheep (1/400, Invitrogen, Mulgrave,

Australia) in BS for 2 hours at 20^{O}C. Sections were washed, mounted and coverslipped in fluorescent mounting medium (Dako).

Iba-1/BrdU: Floating sections were washed in PBS then incubated in 2 M HCl at 37^{O}C for 30 minutes. After extensive PBS washes sections were incubated in BS for 1 hour at 20^{O}C, then in rabbit anti-Iba-1 (1/300, Wako) and sheep anti-BrdU (1/500, Exalpha) in BS, O/N at 20^{O}C. Sections were then washed in PBS and incubated in CY3-conjugated donkey anti-sheep (1/300, Jackson Immunoresearch) and Alexa Fluor 488-conjugated donkey anti-rabbit (1/300, Invitrogen) in BS for 2 hours at 20^{O}C. Sections were washed, mounted and coverslipped in fluorescent mounting medium (Dako).

mHtt double-labeling: The EM48 clone mouse monoclonal antibody (Merck-Millipore) was used to detect mHtt protein aggregates (H. Li et al. 2003). Immunoreactivity was never observed in wildtype sections using the EM48 antibody (data not shown). Sections for mHtt /BrdU labeling were placed into 2 M HCL for 30 minutes at 20^{O}C then washed extensively. All sections were then placed into BS for 1 hour at 20^{O}C and then incubated O/N at 20^{O}C with mouse anti-huntingtin (EM48, 1/300, Merck-Millipore) and either; sheep anti-BrdU (1/500, Exalpha), rabbit anti-Ki67 (1/200, Lab Vision), rabbit anti-c-Fos (1/300, Santa Cruz Biotechnology), rabbit anti-GFAP (1/500, Dako), rabbit anti-Iba-1 (1/300, Wako) or biotinylated lycopersicon esculentum (Lectin, 1/1000, Vector Laboratories). Sections were then washed in PBS, placed into respective fluorescent secondary antibody combination; CY3-conjugated donkey anti-mouse (1/400, Jackson ImmunoResearch) and Alexa Fluor 488-conjugated donkey anti-rabbit (1/400, Invitrogen) or Alexa Fluor 488-conjugated donkey anti-mouse (1/400, Invitrogen) and CY3-conjugated streptavidin (for the lectin double label, 1/500, Jackson ImmunoResearch) for 2 hours at 20^{O}C. Sections were washed, mounted and coverslipped in fluorescent mounting medium (Dako).

NeuN/BrdU/c-Fos: Sections were washed in PBS then incubated in 2 M HCl at 37^{O}C for 30 minutes. After extensive washing in PBS sections were incubated in BS for 1 hour at 20^{O}C followed by BS containing mouse anti-NeuN (1/300, Merck-Millipore) O/N at 20^{O}C. Washed sections were then incubated for 2 hours at 20^{O}C in Alexa Fluor 594-conjugated donkey anti-mouse (1/400, Invitrogen). Sections were then washed and incubated in both sheep anti-BrdU (1/500, Exalpha) and rabbit anti-c-Fos (1/300, Santa Cruz Biotechnology) O/N at 20^{O}C. Washed sections were then incubated in BS containing both CY3-conjugated donkey anti-sheep (1/300,

Jackson ImmunoResearch) and Alexa Fluor 488-conjugated donkey anti-rabbit (1/400, Invitrogen) 2 hours at 20^{O}C. Sections were washed, mounted and coverslipped in fluorescent mounting medium (Dako).

Multi-label fluorescence counts

Confocal microscopy was employed to count fluorescently double/triple-labeled cells in anatomically matched sections from coded slides as previously described (Ransome & Turnley 2007, 2008). Four serial sections spaced 480μm apart between bregma – 1.34 mm and bregma – 2.70 mm (Paxinos & Franklin 2001) were analyzed per multi-label in each animal. Z-stacks of digital images were captured using a MRC1024 confocal scanning laser system (Bio-Rad, Hercules, USA) installed on a Zeiss Axioplan 2 microscope (Carl Zeiss, North Ryde, Australia) and an Olympus oil immersion 63x objective lens (Olympus). Images were scanned at 2μm intervals (except mHtt co-labeling, which was analyzed exhaustively in 1μm steps) through the extent of the z-axis. A minimum of 5 separate images were used for each double-label per animal. Images were reconstructed in 3-dimensions and analyzed using Image J software (NIH, Bethesda, USA).

Experiment#1: Basal and running-induced cellular proliferation and neuronal differentiation (Figure 1A)

At 12 weeks of age control mice were housed singularly in cages with bedding and nesting material: wildtype (*n*=5 females; *n*=5 males) and R6/1 HD (*n*=5 females; *n*=5 males). Voluntary running mice: wildtype (*n*=6 females; *n*=6 males) and R6/1 HD (*n*=6 females; *n*=6 males) had unlimited access to a metal running wheel of 12cm diameter electronically connected to a counter to measure running distances every 24 hours. All mice were given 24 hours to acclimatize to their respective housing then held in their respective housing conditions for seven days receiving daily intraperitoneal (IP) injections of 5-bromodeoxyuridine (BrdU, 50mg/kg, Sigma-Aldrich). One day after the final BrdU injection mice were deeply anaesthetized by IP Lethabarb (325mg/ml Pentobarbitone Sodium, Virbac, Australia) then intracardially perfused with 0.9% saline followed 4% paraformaldehyde (PFA). Extracted brains were post-fixed in 4% PFA at 4^{o}C for 24 hours then saturated in 20% sucrose (Merck) for 24 hours at 4^{o}C, embedded in Optimal Cutting Temperature compound (Sakura-Finetek, Torrance, USA) and frozen in liquid

Nitrogen-cooled iso-pentane. Serial coronal sections (40μm) were cut on a cryostat from the olfactory bulb to the caudal hippocampus and stored in 0.1 M phosphate buffer (PB) containing 25% ethylene glycol and 25% glycerol (Chem-Supply Pty Ltd, Gillman, Australia) at -20^{O}C until used for immunohistochemistry (above). The density of Ki67(+) and BrdU(+) cells were obtained to measure proliferating precursors in the SGZ. DCX is transiently expressed by maturing SGZ neurons (Brown et al. 2003; Kempermann et al. 2004). 100-140 BrdU(+) cells in the SGZ per mouse were examined for DCX co-labeling to measure neuronal differentiation and results are expressed as the percentage of BrdU(+) cells co-labeled with DCX ± sem. SGZ confocal images from R6/1 HD female standard housed mice were also used to analyze mHtt co-labeling in 30-40 Ki67(+) and 60-70 BrdU(+) cells.

Experiment#2: Basal and running-induced hippocampal Akt activity (Figure 1B)

Twelve-week-old female mice were housed as described for experiment#1 without BrdU injections; standard housing (*n*=5 wildtype; *n*=5 R6/1 HD) or voluntary running (*n*=5 wildtype; *n*=5 R6/1 HD). Animals were euthanized by cervical dislocation and hippocampi rapidly isolated in ice-cold 0.1M Tris buffered saline (TBS) and snap-frozen in liquid nitrogen. Hippocampi were mechanically homogenised on ice in 500μl of RIPA buffer (Cell Signalling Technologies) containing; 20mM Tris-HCl (pH 7.5), 150mM NaCl, 1mM Na_2EDTA, 1mM EGTA, 1% NP-40, 1% sodium deoxycholate, 2.5mM sodium pyrophosphate, 1mM β-glycerophosphate, 1mM Na_3VO_4, 1μg/ml leupeptin with added 0.1% sodium dodecyl sulfate and protease inhibitor cocktail (Roche, Hawthorn, Australia). Samples were allowed to sit on ice for 30 minutes before being centrifuged at 150 x g for 20 minutes at 4^{O}C. Supernatants were collected and protein concentration determined by the Bradford method before the samples were boiled in loading buffer (50mM Tris, pH 6.8; 2% sodium dodecyl sulfate; 0.1% bromophenol blue, 10% glycerol, 100mM DTT[Sigma-Aldrich]). Samples containing 40μg of protein were electrophoretically resolved on 10% poly acrylamide gels (Invitrogen) for 90 minutes at 120 V then transferred to nitrocellulose membrane (Bio-Rad) for 3 hours at a constant 200mA.

Membranes were blocked for 1 hour at 20^{O}C in TBS containing 0.1% Tween-20 (TBS-T) and 5% skim milk powder then incubated in the following primary antibodies at 4^{O}C, overnight; rabbit anti-Akt (1/1000), rabbit anti-Akt phosphorylated at serine residue 473 (pAkt$^{(473)}$; 1/1000), rabbit anti-Insulin like growth factor-1 receptor (IGF-1R, 1/1000), rabbit anti-caspase-3 (all Cell

Signalling Technologies), rabbit anti-Iba-1 (1/500, Wako), rabbit anti-GFAP (1/500, Dako) or mouse anti-β-Actin (Sigma-Aldrich). Following washing in TBS-T, blots were incubated in horseradish peroxidase-linked anti-rabbit IgG or horseradish peroxidase-linked anti-mouse IgG (both 1/5,000, Cell Signaling Technologies) for 2 hours at 20^{O}C, followed by washing in TBS-T. Immunoreactive bands were detected by Pierce SuperSignal West Pico Chemiluminescent Substrate (Thermo Fisher Scientific) and digitally captured using a Gel Document system and VisionWorks®LS software (UVP, Upland, USA). Brightness and contrast were optimized and composite images created using Adobe Photoshop 7.0 and Macromedia Freehand 10.0 software (both Adobe, San Jose, USA). Densitometry analysis was performed on digital images using Image J software (NIH, Bethesda, USA). Images were converted to 8-bit grey scale and the intensity of specific immuno-reactive bands measured using the *Analyse / Gels* tool (http://rsb.info.nih.gov/ij/docs/menus/analyze.html #gels). Specified bands were then compared relatively to their respective β-Actin band density and pAkt$^{(473)}$ compared to total Akt. Results are expressed in arbitrary units as means ± sem.

Experiment#3: Sequential running and enrichment induced mature AHN (Figure 1C)

Expression of c-Fos in surviving mature adult-generated hippocampal neurons was examined in female wildtype (*n*=18) and R6/1 HD (*n*=18) mice as described previously (Tashiro et al. 2007) with minor modification. At 7 weeks of age control littermate mice were standard group housed (*n*=9 wildtypes; *n*=9 R6/1 HD), while group housed run/enriched littermate mice (*n*=9 wildtypes; *n*=9 R6/1 HD) were housed singularly with a running wheel for 7 days (as described in experiment#1). During the last 4 days of running the run/enriched mice received twice daily IP injections of BrdU (50mg/kg, Sigma-Aldrich) spaced 10 hours apart as did control mice in corresponding standard housing. Run/enriched mice were then placed back into group housing for 1 week and then placed into enriched group housing for 1 week (BrdU-labeled cells ranging in age between 7 - 11 days) consisting of plastic tunnels, toys and synthetic climbing ropes. Subsequently run/enriched mice were again returned to standard group housing for another 4 weeks. Run/enriched mice were placed into their exactly replicated enriched environments for 2.5 hours and transcardially perfused over 90 minutes such that individual exposure to enrichment ranged between 2.5-4 hours (Tashiro et al. 2007). Control mice having been standard housed for the same 6-week period were also placed into comparable enriched

cages and similarly perfused. Brains were prepared for immunohistochemistry as described in experiment#1. Cell survival (42 days after BrdU administration) was examined by quantiating BrdU(+) cell density in the GCL. Confocal analysis of 40-60 BrdU(+) cells in the GCL per mouse were examined for NeuN co-labeling as a measure of mature neuronal differentiation (Kempermann et al. 2004) and NeuN/c-Fos triple labeling as an indirect marker of neuronal activity (Tashiro et al. 2007). In each case results are expressed as the mean percentage of BrdU(+) cells co-labeling with NeuN or NeuN/c-Fos ± sem.

Iba-1 is a calcium-binding protein expressed by microglia (Sasaki et al. 2001). Sections from standard housed wildtype and R6/1 HD female mice were used to measure Iba-1(+) cell densities in the SGZ ,GCL and hilus regions. In R6/1 HD female standard house mice SGZ/GCL confocal images were used to analyze mHtt in; 20-30 BrdU(+) cells, 80-100 c-Fos(+) cells, 30-40 GFAP(+) astrocytes and 30-40 Iba(+) micoglia. For Lectin(+) vascular 6-8 images of the SGZ/GCL were analyzed for Lectin/mHtt co-labeling.

Experiment#4 Serum Analysis

Blood was derived via left ventricular puncture under heavy anesthesia from **a forth group of** female wildtype and R6/1 HD mice at 12 weeks of age. Blood was taken at 10 AM in the light (inactive) phase, 10 PM in the dark (active) phase under standard group housing conditions and at 10PM after approximately 2 hours of running in singularly housed cages with running wheel. Blood was allowed to clot overnight at $4^{O}C$, centrifuged at 150 x g for 20 minutes and then supernatant (serum) was collected and stored at $-80^{O}C$ until analyzed. ELISA was used to assay the serum samples for concentrations of TFGβ-1 and IGF-1 (both; R & D Systems, Minneapolis, USA) and GH (Merck-Millipore) in duplicate according to manufacturer's instructions. Data was analyzed using either 4- or 5- parameter logistics curves as per manufacturer's instructions and results are expressed as mean pg/ml or ng/ml ± sem

Statistical Analysis

Data subjected to 3 factor ANOVA were analyzed for statistical significance using SPSS software (SPSS Inc., Chicago, USA) with subsequent multiple pair-wise comparisons made using the Least Significant Difference (LSD) test. Data subjected to 2-tailed unpaired student's t-test and two-way ANOVA were analyzed for statistical significance using GraphPad Prism 5

software (GraphPad Software Inc., San Diego, USA) and the Bonferroni's test was employed for multiple pair-wise comparisons where applicable in two-way ANOVA. Results were considered significant at $P<0.05$.

Results

Voluntary running levels are reduced in R6/1 HD mice

Female and male mice from each genotype placed into voluntary running groups had their wheel activity digitally monitored and recorded daily in the form of distance run / 24-hours over 8 consecutive days (Fig. 2). Daily tracking of running distances showed that female R6/1 HD mice ran consistently less than female wildtype mice, with days 1, 2, 4, 5 and 6 showing significant decreases (Fig. 2A). A similar comparison showed a more severe deficit in voluntary running activity in male R6/1 HD animals compared to male wildtypes (Fig. 2B). Female rodents have previously been shown to engage in higher levels of voluntary running compared to age-matched males (Lightfoot 2008). We therefore performed a 2-factor (genotype x sex) analysis of the 8-day mean running distances / 24 hours (Fig. 2C). Two-way ANOVA statistical analysis showed significant main effects of genotype, $F_{(1,21)}$=18.08; P=0.0004 and sex, $F_{(1,21)}$=35.71; P<0.0001, (Fig. 2C). Bonferroni's pair-wise comparisons revealed males had significant reductions in running distances compared to females in their respective genotypes, while both R6/1 HD female and male mice ran significantly less compared to wildtype mice within each sex (Fig. 2C).

Analysis of proliferating progenitor cells in the SGZ in response to wheel running

A proliferative cascade forms the initial step in AHN and is up-regulated by voluntary running (Kempermann et al. 2004; van Praag et al. 1999a). We assessed Ki67(+) and BrdU(+) cell densities in the SGZ of wildtype and R6/1 HD female and male mice in standard housing and after 8 days of voluntary running (Fig. 3A - C). We performed a 3 factor ANOVA (genotype x sex x housing) statistical analysis that showed no significant changes in the volume of the sampled SGZ (Fig. 3A). Three-way ANOVA statistical comparison of Ki67(+) cell densities (Fig. 3B) showed main effects of genotype, $F_{(1,47)}$=53.64, P<0.001; sex, $F_{(1,47)}$=4.60, P<0.05 and housing, $F_{(1,47)}$=36.87, P<0.001 with a significant interaction between genotype and housing, $F_{(1,47)}$=16.57, P<0.001. Three-way ANOVA comparison of BrdU(+) cell densities 24-hours after the last BrdU injection (Fig. 3C) showed main effects of genotype, $F_{(1,47)}$=67.50, P<0.001; sex, $F_{(1,47)}$=12.18, P<0.005 and housing, $F_{(1,47)}$= 29.09, P<0.001 with significant interactions between genotype and housing, $F_{(1,47)}$=16.57, P<0.001 and sex and housing, $F_{(1,47)}$=6.58, P<0.05. Pair-

wise comparisons were made using the LSD test for both Ki67(+) (rows above dashed line) and BrdU(+) (columns below the dashed line) cell densities shown in table 1. In standard housing; female wildtype and R6/1 HD mice had comparable Ki67(+) cell densities, while male R6/1 HD mice had significantly lower Ki67(+) cell densities compared to wildtype males. Running significantly increased Ki67(+) cells densities in female and male wildtype mice but not in R6/1 HD mice of either sex. There were no sex differences in Ki67(+) cell densities within wildtype standard housed or running groups or between female and male R6/1 HD mice within standard housing. However, female R6/1 HD mice had higher Ki67(+) cell densities compared to R6/1 HD males within the running group.

Bolded *P*-value entries in the BrdU pair-wise comparisons highlight differences in significance compared to corresponding Ki67 pair-wise comparisons in table 1. Of particular note, female R6/1 HD mice had significantly lower BrdU(+) cell densities compared to female wildtype mice within the standard housed group. Within wildtype groups there was no difference between sexes in BrdU(+) cell densities in standard housing, however while running increased BrdU(+) cell densities in females and males, the density of BrdU(+) cells was lower in running males compared to running females. Again there was no significant changes between female and male R6/1 HD mice in standard housing and nor did running increase BrdU(+) cell densities in either sex. However, in contrast to the Ki67(+) cell data, there was no difference between R6/1 HD female and male mice within the running group.

Running promotes early neuronal differentiation in wildtype and R6/1 HD mice

Maturing SGZ progenitors express DCX as a milestone of early neuronal differentiation (Brown et al. 2003; Kempermann et al. 2004). We employed confocal microscopy and BrdU/DCX double-label immunofluorescence to assess neuronal differentiation one day after the final BrdU injection in standard housed and running female and male wildtype and R6/1 HD mice (Fig. 4). Where approximately 50% of the BrdU(+) cells analyzed at this time-point co-labeled with DCX in standard housed wildtype and R6/1 HD mice, a slightly higher proportion was observed in the running groups. Three-way ANOVA statistical analyses (genotype x sex x housing) of the proportion of BrdU(+) cells co-labeling with DCX showed a main effect of housing, $F_{(1,47)}=20.87$, $P<0.001$ (Fig. 4). Multiple pair-wise comparisons using the LSD test are shown in table 2. Within both standard housing and running groups there were no significant

changes in the proportion of BrdU(+) cells co-labeling with DCX between females and males within either genotype. Of note, R6/1 HD male running mice had higher proportions of BrdU/DCX co-labeling compared to R6/1 HD standard housed males, despite very low running distances.

Synergistic stimulation of AHN and c-Fos expression in female R6/1 HD mice

Male R6/1 HD mice had ostensibly no voluntary running activity despite a similar relative sex difference within genotypes. Together with no apparent R6/1 HD sex difference in proliferation, this would introduce considerable variation. We therefore focused the remainder of the study on female mice. Voluntary running and enriched environments facilitate enhanced AHN through distinct pathways of cell proliferation and cell survival, respectively (Olson et al. 2006). We hypothesized that a combinatorial approach of sequential voluntary running followed by environmental enrichment would increase AHN in R6/1 HD female mice. Again R6/1 HD female mice engaged in significantly lower voluntary running activity over a one-week period, with mean daily distances of; wildtype, 10,009±1,142 meters/24 hours and R6/1 HD, 5,886±843 metres/24 hours; $P<0.05$, student's 2-tailed unpaired t-test. However, both wildtype and R6/1 HD female mice were qualitatively observed to actively explore their enriched environments consistently over the subsequent 7-day enrichment period.

Neurons generated within the adult SGZ migrate into the adjacent GCL and show persistent survival rates from one month onwards (Kempermann et al. 2003). Two-way ANOVA (genotype x housing) was used to analyze the density of immunohistochemically identified surviving BrdU(+) cells 42 days after final BrdU injections in female wildtype and R6/1 HD standard housed and running/enriched groups (Fig. 5A). We observed no change in the volume of sampled GCL between any of the groups (Fig. 5B). However, two-way ANOVA examination of surviving BrdU(+) cell densities showed a significant main effect of sequential running/enrichment, $F_{(3,28)}=54.21$, $P<0.0001$, (Fig. 5C). Bonferroni's pair-wise comparisons showed a significant increase in surviving BrdU(+) cell densities in female running/enriched wildtype mice compared to wildtype standard housed and compared to both R6/1 HD standard housed and R6/1 HD running/enriched mice (Fig. 5C). Despite sequential voluntary running and environmental enrichment doubling the density of surviving BrdU(+) cells in R6/1 HD mice, the increase was not statistically significant in pair-wise Bonferroni's analysis. However, while

female wildtype standard housed mice had significantly higher surviving BrdU(+) cell densities compared to R6/1 HD standard housed females, this significance was abolished when wildtype standard housed mice were compared to R6/1 HD running/enriched mice (Fig. 5C).

We next **examined co-expression of the** mature neuronal marker NeuN and the indirect marker of neuronal activation c-Fos (Tashiro et al. 2007). We employed triple-label immunofluorescence and confocal microscopy to determine the proportion of surviving BrdU(+) cells that were mature neurons (BrdU/NeuN co-labeled; (van Praag et al. 1999b) and activated mature neurons (BrdU/NeuN/c-Fos co-labeled; (Tashiro et al. 2007) (Fig. 5D - F). In all groups analyzed we observed approximately 80% of the BrdU(+) cells adopting a mature neuronal phenotype as evidenced by their co-expression of NeuN (Fig. 5D), suggesting that mature neuronal differentiation was unaffected in the adult GCL of female R6/1 HD mice. However, taken together with the BrdU(+) cell density analysis (Fig. 5C), net neurogenesis in female R6/1 HD mice is decreased compared to female wildtype mice. Introducing naive standard housed mice and reintroducing the running/enriched mice to enriched housing for an acute period prior to perfusion enables the assessment of experience-specific **neuronal activity** through BrdU/NeuN/c-Fos co-labeling (Tashiro et al. 2007). Performing this analysis found no significant changes in proportions of BrdU(+) cells co-labeling with NeuN/c-Fos in female wildtype and R6/1 HD mice (Fig. 5F).

Akt signaling is altered in the hippocampus of female R6/1 HD mice

According to the somatomedin hypothesis, pituitary-derived GH stimulates hepatic secretion of IGF-1 into the circulation (Rotwein 2012) and serum IGF-1 mediates running-induced AHN (Trejo et al. 2007). Therefore, we next examined serum concentrations of GH and IGF-1 in female wildtype and R6/1 HD mice (Fig. 6A - B). Endocrine-derived GH/IGF-1 is subject to diurnal rhythm so that we assessed serum samples obtained from mice in standard housing during the day, standard housing at night and also after 2 hours of voluntary running at night. Two-way ANOVA (genotype x housing) was used to assess serum concentrations of GH demonstrating a main effect of housing; $F_{(2,24)}=12.64$, $P<0.0005$, (Fig. 6A), with Bonferroni's pair-wise comparisons showing that serum GH concentrations remained unchanged between female wildtype and R6/1 HD mice in day-time and night-time standard housing, while acute voluntary running induced similar significant increases in both genotypes (Fig. 6A). The same

serum samples were examined in parallel for IGF-1 concentrations with 2-way ANOVA showing a significant interaction between genotype and housing; $F_{(2,24)}$=6.43, P<0.01 and main effect of housing; $F_{(2,24)}$=6.43, P<0.01, (Fig. 6B). Bonferroni's pair-wise comparisons demonstrated that acute voluntary running increased serum IGF-1 concentrations compared to day-time standard housed female wildtype mice only, while day-time standard housed female R6/1 HD mice had higher serum IGF-1 concentrations compared to standard housed day-time wildtypes. A prominent IGF-1 signal transduction pathway through the IGF-1 receptor (IGF-1R) propagates signals through Akt phosphorylation (Annunziata et al. 2011). We used Western blot to quantify IGF-1R as well as total and phosphorylated Akt protein levels in hippocampi derived from female wildtype and R6/1 HD mice in standard housing and after 8 days of voluntary running (Fig. 6C-D). Again female R6/1 HD mice engaged in significantly lower levels of voluntary running compared to female wildtypes, with mean daily distances of; 11,845±1,269 meters/24 hours, wildtype versus 6,097±953 meters/24 hours R6/1 HD; P<0.01, 2-tailed unpaired student's t-test. While hippocampal IGF-1R protein levels were unchanged between any of the groups using 2-way ANOVA (genotype x housing; Fig. 5C), we observed a significant main effect of running on Akt phosphorylation ($pAkt^{(473)}$) levels compared to total Akt, $F_{(1,16)}$=7.14, P<0.05, with Bonferroni's pair-wise comparisons showing running induced Akt phosphorylation in female wildtypes, but not R6/1 HD mice (Fig. 6D). We further observed a main genotype effect on total levels of Akt, $F_{(1,16)}$=28.83, P<0.0001, with Bonferroni's pair-wise comparisons showing female R6/1 HD mice had reduced levels compared to wildtypes within both standard and running housing (Fig. 6D). Postmortem brain analyses have found reduced Akt levels in HD patients possibly attributed to caspase-3 activity (Colin et al. 2005). Western blotting was unable to detect caspase-3 in hippocampi from female wildtype and R6/1 HD standard housed and running mice (not shown). We further used immunohistochemistry to quantify caspase-3(+) cell densities in the SGZ/GCL and found no change between any of the groups (Fig. 6E).

Female R6/1 HD mice do not show overt activation of hippocampal microglia

Circulating TGFβ levels are reduced in HD patients (Battaglia et al. 2011), while increased TGFβ-signaling may inhibit AHN in HD transgenic rats (Kandasamy et al. 2010). We used the same serum samples derived for the analyses of GH/IGF-1 concentrations (Fig. 6A-B) and measured TGFβ by ELISA (Fig. 7A). Two-way ANOVA (genotype x housing)

demonstrated a main effect of housing, $F_{(2,24)}$=5.96, P<0.05, with Bonferroni's pair-wise comparisons showing a significant increase in serum TGFβ concentrations in female wildtype night-time standard housed mice compared to female wildtype running mice (Fig. 7A). The reduced serum TGFβ concentrations in female R6/1 HD mice compared to wildtypes in day-time standard housing did not reach significance. TGFβ actions on microglia may be a key influential factor regulating AHN (Abutbul et al. 2012; Morrens et al. 2012). We employed double-label immunofluorescence and confocal microscopy to examine for evidence of microglia activation through proliferation. However, the proportion of BrdU(+) cells co-labeling with Iba-1(+) microglia remained unchanged between female wildtype and R6/1 HD standard housed mice (Fig. 7B). Iba-1 immunohistochemistry was used to examined microglia density in the GCL, SGZ and hilus regions of the hippocampus and revealed a significant decrease in Iba-1(+) cell density in the GCL of female R6/1 HD mice compared to wildtypes in standard housing ($t_{(8)}$=2.901; P<0.05), while no changes were evident in the SGZ or hilus regions (Fig. 7C). Microglial up-regulation of Iba-1 (Sasaki et al. 2001) and astrocyte up-regulation of GFAP (Silver & Miller 2004) can be coincident with neuroinflammation that could suppress AHN. However, Western blot analyses found no change in total hippocampal protein levels of Iba-1 (Fig. 7D) or GFAP (Fig. 7E) between standard housed female wildtype and R6/1 HD mice.

mHtt-containing protein aggregates appear restricted to existing mature neurons in standard housed female R6/1 HD mice

Intraneuronal protein aggregates containing mHtt are a pathological hallmark of HD and can be detected with a monoclonal antibody (H. Li et al. 2003). Over 300 Ki67(+) cells were analyzed in the SGZ of standard housed female R6/1 HD mice and were never found to harbor mHtt aggregates (Fig. 8A). BrdU(+) cells analyzed one day after the final BrdU injection in standard housed female R6/1 HD mice ranged in age from one to seven days and again we failed to observe any mHtt aggregates in this population (Fig. 8B). BrdU(+) cells detected 42-days after BrdU labeling had migrated into the GCL where the density of immunofluorescent mHtt aggregates was high. High resolution 3-demensional reconstruction of confocal images of BrdU/mHtt co-labeling using 1μm optical slices at 1μm intervals through the z-axis showed BrdU-labeled nuclei in close proximity to mHtt-labeled aggregates but were never found to co-labeled (Fig. 8C). Given we examined functional AHN through c-Fos expression, we next

analyzed c-Fos(+) cells in the GCL of standard housed female R6/1 HD mice. High resolution 3-demensional confocal reconstructions found a relatively consistent proportion of c-Fos/mHtt co-labeled cells over 6 individual female R6/1 HD mice (Fig. 8D), with a mean proportion of 58.8 ± 1.7% of c-Fos(+) cells displaying mHtt aggregates. The neurogenic niche, populated with astrocytes, endothelium and microglia, is postulated to orchestrate the regulation of AHN (Williams & Lavik 2009). The notion that this niche may play a causative role in HD-mediated AHN deficits (Phillips et al. 2005) prompted us to further analyze mHtt aggregates. Despite the dense staining in the GCL, careful confocal scrutiny failed to detect mHtt immunoreactive aggregates in vascular endothelium (Fig. 8E), GFAP(+) astrocytes (Fig. 8F) or Iba-1(+) microglia (Fig. 8G).

Discussion

The cellular and molecular mechanisms that underlie HD pathophysiology are not fully understood. Several HD mouse models exhibit AHN deficits, which if restored, could provide therapeutic efficacy dependent on the ability of these adult-generated neurons to functional integrate (Ransome et al. 2012). Furthermore, accumulating evidence points toward sexual dimorphism in HD behavioral deficits in which AHN may play a role (Ransome et al. 2012). Hence, our current study examined the response of female and male R6/1 HD mice to running-induced precursor proliferation and further examine evidence **of c-Fos expression in** adult generated mature hippocampal neurons.

Previous reports have demonstrated that independent transgenic mouse HD models are refractory to running-induced AHN (Kohl et al. 2007; Potter et al. 2010). Despite isolated male N171-82Q transgenic mice engaging in comparable running distances to their wildtype controls, AHN deficits were not rescued (Potter et al. 2010). In another study, AHN was not stimulated in female R6/2 transgenic mice group housed with running wheels, though distances in this study were not directly measured (Kohl et al. 2007). Reflecting these two studies our transgenic mice were motor asymptomatic and of good general health at the onset of running activity. However, we used a shorter duration of exercise based on studies showing that by 3 weeks of continuous running the stimulatory effect on precursor proliferation is lost (Clark et al. 2010). Although voluntary running potently stimulates AHN (van Praag et al. 1999a), a significant confound in our current study resides in the dramatically decreased running distances in the R6/1 HD mice. A well documented sex-bias in rodent voluntary running activity links higher running distances in females with higher estradiol levels compared to males (Lightfoot 2008). While this sex-bias was reflected in our current study within both genotypes, the male R6/1 HD mice had almost negligible voluntary running activity. Several independent cohorts of R6/1 HD female and male mice used in this study showed similar reductions, which argues against a chance phenotypic observation.

Reduced serum concentrations of sex-hormones could potentially explain the observed reduced running activity (Lightfoot 2008). Male HD patients have reduced serum testosterone concentrations (Markianos et al. 2005) as do male R6/1 HD mice at an age equivalent to the mice used in this study (Hannan & Ransome 2012; Ransome 2012). Whether female HD patients and

female R6/1 HD mice have lowered circulating estradiol remains to be explored as does the ability of hormone therapy to restore voluntary running activity in the R6/1 model. Social isolation is another potential confounding factor in our study, where mice were singularly housed to ensure accurate measures of running distances. We have shown that female R6/1 HD mice have exacerbated stress responses compared to R6/1 HD males (Du et al. 2012). We would therefore anticipate isolation to impact the running distances of female R6/1 mice more than males, which is in contrast to our results. Additionally, isolation did not affect exercise-induced precursor proliferation in either female or male wildtype mice, although such an effect has been reported in rats (Leasure & Decker 2009). A fuller exploration of circulating stress and sex hormones in relation to voluntary running is warranted, particularly with regard to the growing acceptance that an inactive lifestyle predicts earlier onset and more rapid symptom progression for HD patients (Trembath et al. 2010).

Significant interest also exists into the regulation of AHN and hippocampal-related behaviour by sex hormones (Galea et al. 2008). Estradiol appears to stimulate proliferation of hippocampal neuronal precursors, while testosterone and dihydrotestosterone promote survival of newly generated neurons (Galea 2008). Estrous cycle and flux of circulating estradiol levels could affect proliferation rates of neuronal precursors as could a hypothesized reduction in serum oestrogens in female R6/1 HD mice. Ki67 is an intrinsic marker of cell proliferation expressed during all active cell-cycle phases and provides a 'snap-shot' of mitotic activity (Kee et al. 2002; Scholzen & Gerdes 2000), while exogenous BrdU is incorporated into cellular DNA during synthesis-phase and allows tracing of cells over time. Ki67(+) cell densities showed a proliferation deficit in male but not female R6/1 HD mice when compared to sex-matched wildtypes under standard housing. In contrast, R6/1 HD mice of both sexes showed a deficit in BrdU(+) cell densities. The BrdU analyses of proliferation occurring 1 day after 7 days of consecutive BrdU administration results in an accumulative effect as BrdU is passed on to progeny and also incorporates short-term survival since the BrdU(+) cells range in age from 1 to 7 days. These variables could explain why the BrdU deficits were more marked compared to the Ki67 data, where cell cycle kinetics or cellular survival are affected by HD. Neither Ki67 nor BrdU data showed any change between housing-matched females and males within genotypes, which accords with our previous examination of hippocampal precursor proliferation in female and male mice (Manning et al. 2012). Moreover, our results do not suggest that SGZ precursor

proliferation was affected by estrous cycle or the potential of HD-mediated reductions in circulating estradiol.

We were unable to stimulate proliferation in either sex of R6/1 HD mice with voluntary running. This failure would be anticipated in the male group given the negligible engagement in running activity. However, previous studies showing a positive correlation between running distances and increased precursor proliferation (Allen et al. 2001), suggest the female R6/1 HD mice might have remained proportionally responsive. While we did observe an increase in both Ki67 and BrdU cell densities in the R6/1 HD female running mice compared to sex and genotyped matched standard housed mice, the increase did not reach statistical significance. We have previously shown that female but not male R6/1 HD mice up-regulate hippocampal brain derived neurotrophic factor (BDNF) in response to voluntary running (Zajac et al. 2010). Our current quantitative data on running distances may explain this observation. Recent evidence suggests that voluntary running provides the major stimulatory effect in enrichment paradigms that incorporate running wheels designed to promote AHN, BDNF expression and hippocampal-dependent cognition (Kobilo et al. 2011; Mustroph et al. 2012). These findings together with our current results highlight the importance of careful design and interpretation of R6/1 HD experiments using mixed sexes and enriched environments containing running wheels.

Running-induced AHN may be mediated by concomitant increases in hippocampal BDNF expression (Kobilo et al. 2011). However, since female R6/1 HD mice elevate hippocampal BDNF in response to voluntary running (Zajac et al. 2010) we explored other potential deficits that could prevent running-induced AHN. Elevated TGFβ1 in HD could inhibit AHN directly or through activating local glial cells and up-regulating GFAP expression (Kandasamy et al. 2010; Sapp et al. 2001; Silver & Miller 2004; Tai et al. 2007; Wachs et al. 2006). However, we found no evidence to support such changes in R6/1 HD female mice. We did find reduced microglia density in the GCL of the R6/1 HD mice, which could conceivably contribute to AHN deficits through reduced trophic cytokine secretion (Ekdahl et al. 2009; Kempermann & Neumann 2003). Based on known neuroendocrine dysfunction in HD (Hult et al. 2010; Petersen & Bjorkqvist 2006), we hypothesized that abnormal GH/IGF-1 serum levels in R6/1 HD mice may block running-induced AHN. This rationale is underpinned by studies showing IGF-1 derived from the liver crosses the blood-brain-barrier to up-regulate AHN in response to voluntary running (Trejo et al. 2001). Liver derived IGF-1 is primarily under the

regulation of pituitary GH and together are subject to diurnal rhythm (Rotwein 2012). Previous studies have shown IGF-1 serum concentration initially rise before progressively falling with running wheel activity (Ploughman et al. 2005). Taking these observations into account we examined serum concentrations of GH and IGF-1 after a single 2 hour bout of running wheel activity. Of note, despite reduced running distances, the female R6/1 HD mice responded by increasing serum GH to a similar level observed in running wildtype mice. This running-induced increase was not reflected by an increase in serum IGF-1. This may be attributed to the necessity of GH to induce hepatic IGF-1 gene transcription, maturation and secretion, which had not taken place at the time we derived serum. Reductions in serum IGF-1 with longer running periods is postulated to reflect tissue (including brain) uptake (Ploughman et al. 2005). An alternative explanation therefore, is that our timing of serum extraction missed the initial serum IGF-1 rise in response to running activity. Further analyses at multiple time-points after the onset of running will be required to establish whether serum IGF-1 decreases in R6/1 mice as an indicator of tissue up-take. It remains plausible that brain up-take of circulating IGF-1 is impaired in R6/1 HD mice, which would be anticipated to reduce IGF-1 mediated cellular signalling.

Signaling by IGF-1 is mediated through the IGF-1R and utilizes the Akt cell-survival pathway important in running-induced AHN (Bruel-Jungerman et al. 2009; Franke et al. 2003). Levels of hippocampal IGF-1R remained unchanged in R6/1 HD female mice under control housing and after 8 days of voluntary running compared to matched wildtypes. In contrast however, after 8-days of voluntary running phosphorylated Akt levels (an index of Akt activation) were increased in wildtype but not R6/1 HD mice. Again, in conjunction with serum IGF-1 measurements, our data would be underpinned by further studies examining whether acute running periods can induce activated Akt in R6/1 HD mice. **Further examination of how periods of environmental enrichment affect circulating IGF-1 levels and central Akt phosphorylation will be needed to discern whether R6/1 are refractory to exercise soley or more generally to physiological or pharmacological stimulator of the Akt.** Nonetheless, it is possible that failed Akt-mediated signaling observed in this study may underlie the refractory nature of R6/1 HD mice to running-induced AHN. Although Akt phosphorylation levels under standard housing were similar between genotypes, the observation is confounded by the reduced level of total Akt in R6/1 HD female mice. Therefore in absolute terms, basal phosphorylation of hippocampal Akt is reduced in R6/1 HD mice and could also conceivably underlie the basal

AHN deficits. Further experiments analyzing SGZ-specific Akt signaling or *in vitro* analyses of hippocampal precursors will be required to establish a cause and effect relationship. This will be an important endeavour to pursue given that IGF-1/Akt signaling can ameliorate mHtt toxicity (Humbert et al. 2002). Furthermore, postmortem analysis has shown reduced Akt levels in HD-affected brains, thought to be a consequence of caspase-3 activity (Colin et al. 2005). However, our current study found no changes in the density of hippocampal cells expressing activated caspase-3 in R6/1 female HD mice.

We sought to determine whether residual AHN in R6/1 HD mice is functional, which would strengthen the rationale of therapeutically restoring deficits. We combined this endeavour with a novel attempt to increase AHN in R6/1 HD mice by sequentially combining voluntary running and environmental enrichment. Running and enrichment stimulate AHN through independently targeting precursor proliferation and subsequent neuronal survival, respectively (Olson et al. 2006). In these experiments we analyzed BrdU-labeled cells 42 days after administration to determine net neurogenesis and examine whether mature adult-generated neurons express c-Fos as an indirect marker of neuronal activation (Tashiro et al. 2007). The sequential provision of running followed by enrichment markedly increased mature neuronal survival in wildtype but not R6/1 HD female mice. Previous studies demonstrating an additive effect of sequential running and enrichment on AHN increases used a longer enrichment period compared to our current study (Fabel et al. 2009). **Previous studies showing environmental enrichment enhanced survival of adult-generated hippocampal neurons R6/1 mice are limited by not being able to distinguishing between sex, age or duration of enrichment - dependent effects (Lazic et al. 2006).** It remains possible that R6/1 HD mice may respond to an elongated strategy of sequential running/enrichment. Neuronal differentiation was unaffected in the R6/1 HD mice, such that reduced neuronal survival primarily underlies AHN deficits. This again would be consistent with reduced Akt-signaling. Importantly, following the methodology of (Tashiro et al. 2007) we observed adult-generated neurons expressing c-Fos in R6/1 HD mice as an indirect marker **of neuronal activity.**

The development of aggregates containing mHtt protein is a pathological hallmark of both clinical HD and transgenic models (Arrasate & Finkbeiner 2011). While aggregates were detected in female R6/1 HD mice, adult-generated neurons were aggregate-free for at least their initial 6 weeks. The adult neurogenic niche is populated by endothelium, astrocytes and

microglia is postulated to orchestrate the regulation of AHN (Williams & Lavik 2009). These cell types were also found to be devoid of aggregates containing mHtt. Debate surrounds the pathological role of protein aggregates in HD, including a possible neuro-protective effect for neurons in which aggregates develop (Arrasate et al. 2004). However, our data suggests that intrinsic cellular dysfunction caused by aggregated protein has no role in the AHN deficits. We have not ruled-out a pathological role for soluble mHtt or micro-aggregates of a size too small for immuno-detection by our current methodology. Furthermore, our confocal reconstruction methodology showed aggregated mutant Huntingtin in close proximity to BrdU-labeled nuclei and *in vitro* cellular analyses or electron microscopy would provide further evidence of mHtt aggregation in adult-generated neurons. We did find c-Fos positive cells in the GCL containing aggregates and our study does not rule out their eventual development in adult-generated neurons.

Conclusion

Our current data extends previous studies examining AHN deficits in R6/1 HD mice. We showed that proliferation of hippocampal neural precursors is impaired equally in female and male R6/1 HD mice. While both sexes of R6/1 HD mice have reduced voluntary running activity, the deficits were more severe in males. Reduced running distances could partly explain the attenuated and non-significant running-induced AHN in female R6/1 HD mice, with reduced hippocampal Akt activity being a potential molecular mediator. Specifically targeting precursor proliferation then neuronal survival through sequential running and enrichment failed to significantly increase AHN in female R6/1 HD mice. However, we demonstrated **mature neurons express the indirect neural activity marker c-Fos**, underpinning the rationale of studies, e.g. (Grote et al. 2005), endeavoring to restore AHN to ameliorate HD symptoms such as cognitive deficits.

Acknowledgements & Funding Source:

National Health and Medical Research Council **Project Grant Number:** 509031 (AJH)

MIR is supported by a National Health and Medical Research Council Australian Biomedical Fellowship (ID: 628868) and AJH is supported by a Australian Research Council Future Fellowship and is an Honorary National Health and Medical Research Council Senior Research Fellow. The funders had no role in study design, data collection and analysis, decision to publish or manuscript preparation.

Conflict of Interest:

There are no conflicts of interest.

References

Abutbul, S., et al., 2012. TGF-beta signaling through SMAD2/3 induces the quiescent microglial phenotype within the CNS environment. Glia. 60, 1160-71.

Allen, D. M., et al., 2001. Ataxia telangiectasia mutated is essential during adult neurogenesis. Genes Dev. 15, 554-66.

Annunziata, M., Granata, R., &Ghigo, E., 2011. The IGF system. Acta Diabetol. 48, 1-9.

Arrasate, M. & Finkbeiner, S., 2011. Protein aggregates in Huntington's disease. Exp Neurol.

Arrasate, M., et al., 2004. Inclusion body formation reduces levels of mutant huntingtin and the risk of neuronal death. Nature. 431, 805-10.

Battaglia, G., et al., 2011. Early defect of transforming growth factor beta1 formation in Huntington's disease. J Cell Mol Med. 15, 555-71.

Borrell-Pages, M., et al., 2006. Huntington's disease: from huntingtin function and dysfunction to therapeutic strategies. Cell Mol Life Sci. 63, 2642-60.

Brown, J. P., et al., 2003. Transient expression of doublecortin during adult neurogenesis. J Comp Neurol. 467, 1-10.

Bruel-Jungerman, E., et al., 2009. Inhibition of PI3K-Akt signaling blocks exercise-mediated enhancement of adult neurogenesis and synaptic plasticity in the dentate gyrus. PLoS One. 4, e7901.

Cattaneo, E., Zuccato, C., &Tartari, M., 2005. Normal huntingtin function: an alternative approach to Huntington's disease. Nat Rev Neurosci. 6, 919-30.

Clark, P. J., et al., 2010. Adult hippocampal neurogenesis and c-Fos induction during escalation of voluntary wheel running in C57BL/6J mice. Behav Brain Res. 213, 246-52.

Clelland, C. D., Barker, R. A., &Watts, C., 2008. Cell therapy in Huntington disease. Neurosurg Focus. 24, E9.

Colin, E., et al., 2005. Akt is altered in an animal model of Huntington's disease and in patients. Eur J Neurosci. 21, 1478-88.

Davies, S. W., et al., 1997. Formation of neuronal intranuclear inclusions underlies the neurological dysfunction in mice transgenic for the HD mutation. Cell. 90, 537-48.

Du, X., et al., 2012. Environmental enrichment rescues female-specific hyperactivity of the hypothalamic-pituitary-adrenal axis in a model of Huntington's disease. Transl Psychiatry. 2, e133.

Ekdahl, C. T., Kokaia, Z., &Lindvall, O., 2009. Brain inflammation and adult neurogenesis: the dual role of microglia. Neuroscience. 158, 1021-9.

Fabel, K., et al., 2009. Additive effects of physical exercise and environmental enrichment on adult hippocampal neurogenesis in mice. Front Neurosci. 3, 50.

Franke, T. F., et al., 2003. PI3K/Akt and apoptosis: size matters. Oncogene. 22, 8983-98.

Galea, L. A., 2008. Gonadal hormone modulation of neurogenesis in the dentate gyrus of adult male and female rodents. Brain Res Rev. 57, 332-41.

Galea, L. A., et al., 2008. Endocrine regulation of cognition and neuroplasticity: our pursuit to unveil the complex interaction between hormones, the brain, and behaviour. Can J Exp Psychol. 62, 247-60.

Gil-Mohapel, J., et al., 2011. Neurogenesis in Huntington's disease: can studying adult neurogenesis lead to the development of new therapeutic strategies? Brain Res. 1406, 84-105.

Gil, J. M. & Rego, A. C., 2009. The R6 lines of transgenic mice: a model for screening new therapies for Huntington's disease. Brain Res Rev. 59, 410-31.

Gil, J. M., et al., 2004. Asialoerythropoietin is not effective in the R6/2 line of Huntington's disease mice. BMC Neurosci. 5, 17.

Gil, J. M., et al., 2005. Reduced hippocampal neurogenesis in R6/2 transgenic Huntington's disease mice. Neurobiol Dis. 20, 744-51.

Grote, H. E., et al., 2005. Cognitive disorders and neurogenesis deficits in Huntington's disease mice are rescued by fluoxetine. Eur J Neurosci. 22, 2081-8.

Hannan, A. J. & Ransome, M. I., 2012. Deficits in spermatogenesis but not neurogenesis are alleviated by chronic testosterone therapy in R6/1 Huntington's disease mice. J Neuroendocrinol. 24, 341-56.

Hatters, D. M., 2008. Protein misfolding inside cells: the case of huntingtin and Huntington's disease. IUBMB Life. 60, 724-8.

HDCRG, 1993. A novel gene containing a trinucleotide repeat that is expanded and unstable on Huntington's disease chromosomes. The Huntington's Disease Collaborative Research Group. Cell. 72, 971-83.

Hult, S., et al., 2010. Hypothalamic and neuroendocrine changes in Huntington's disease. Curr Drug Targets. 11, 1237-49.

Humbert, S., et al., 2002. The IGF-1/Akt pathway is neuroprotective in Huntington's disease and involves Huntingtin phosphorylation by Akt. Dev Cell. 2, 831-7.

Kandasamy, M., et al., 2010. Stem cell quiescence in the hippocampal neurogenic niche is associated with elevated transforming growth factor-beta signaling in an animal model of Huntington disease. J Neuropathol Exp Neurol. 69, 717-28.

Kee, N., et al., 2002. The utility of Ki-67 and BrdU as proliferative markers of adult neurogenesis. J Neurosci Methods. 115, 97-105.

Kempermann, G. & Neumann, H., 2003. Neuroscience. Microglia: the enemy within? Science. 302, 1689-90.

Kempermann, G., Kuhn, H. G., &Gage, F. H., 1997. More hippocampal neurons in adult mice living in an enriched environment. Nature. 386, 493-5.

Kempermann, G., et al., 2004. Milestones of neuronal development in the adult hippocampus. Trends Neurosci. 27, 447-52.

Kempermann, G., et al., 2003. Early determination and long-term persistence of adult-generated new neurons in the hippocampus of mice. Development. 130, 391-9.

Kobilo, T., et al., 2011. Running is the neurogenic and neurotrophic stimulus in environmental enrichment. Learn Mem. 18, 605-9.

Kohl, Z., et al., 2007. Physical activity fails to rescue hippocampal neurogenesis deficits in the R6/2 mouse model of Huntington's disease. Brain Res. 1155, 24-33.

Lafenetre, P., et al., 2011. The beneficial effects of physical activity on impaired adult neurogenesis and cognitive performance. Front Neurosci. 5, 51.

Lazic, S. E., et al., 2004. Decreased hippocampal cell proliferation in R6/1 Huntington's mice. Neuroreport. 15, 811-3.

Lazic, S. E., et al., 2006. Neurogenesis in the R6/1 transgenic mouse model of Huntington's disease: effects of environmental enrichment. Eur J Neurosci. 23, 1829-38.

Leasure, J. L. & Decker, L., 2009. Social isolation prevents exercise-induced proliferation of hippocampal progenitor cells in female rats. Hippocampus. 19, 907-12.

Li, H., et al., 2003. Abnormal association of mutant huntingtin with synaptic vesicles inhibits glutamate release. Hum Mol Genet. 12, 2021-30.

Li, J. Y., Popovic, N., &Brundin, P., 2005. The use of the R6 transgenic mouse models of Huntington's disease in attempts to develop novel therapeutic strategies. NeuroRx. 2, 447-64.

Lightfoot, J. T., 2008. Sex hormones' regulation of rodent physical activity: a review. Int J Biol Sci. 4, 126-32.

Mangiarini, L., et al., 1996. Exon 1 of the HD gene with an expanded CAG repeat is sufficient to cause a progressive neurological phenotype in transgenic mice. Cell. 87, 493-506.

Manning, E. E., et al., 2012. Increased adult hippocampal neurogenesis and abnormal migration of adult-born granule neurons is associated with hippocampal-specific cognitive deficits in phospholipase C-beta1 knockout mice. Hippocampus. 22, 309-19.

Markianos, M., et al., 2005. Plasma testosterone in male patients with Huntington's disease: relations to severity of illness and dementia. Ann Neurol. 57, 520-5.

Morrens, J., Van Den Broeck, W., &Kempermann, G., 2012. Glial cells in adult neurogenesis. Glia. 60, 159-74.

Mustroph, M. L., et al., 2012. Aerobic exercise is the critical variable in an enriched environment that increases hippocampal neurogenesis and water maze learning in male C57BL/6J mice. Neuroscience. 219, 62-71.

Nithianantharajah, J., et al., 2008. Gene-environment interactions modulating cognitive function and molecular correlates of synaptic plasticity in Huntington's disease transgenic mice. Neurobiol Dis. 29, 490-504.

Olson, A. K., et al., 2006. Environmental enrichment and voluntary exercise massively increase neurogenesis in the adult hippocampus via dissociable pathways. Hippocampus. 16, 250-60.

Pang, T. Y., et al., 2006. Differential effects of voluntary physical exercise on behavioral and brain-derived neurotrophic factor expression deficits in Huntington's disease transgenic mice. Neuroscience. 141, 569-84.

Paxinos, G & Franklin, K.B.J. (2001), *The Mouse Brain in Stereotaxic Coordinates* (2nd edn.; San Diego: Academic Press).

Petersen, A. & Bjorkqvist, M., 2006. Hypothalamic-endocrine aspects in Huntington's disease. Eur J Neurosci. 24, 961-7.

Phillips, W., Morton, A. J., &Barker, R. A., 2005. Abnormalities of neurogenesis in the R6/2 mouse model of Huntington's disease are attributable to the in vivo microenvironment. J Neurosci. 25, 11564-76.

Ploughman, M., et al., 2005. Endurance exercise regimens induce differential effects on brain-derived neurotrophic factor, synapsin-I and insulin-like growth factor I after focal ischemia. Neuroscience. 136, 991-1001.

Potter, M., et al., 2010. Exercise is not beneficial and may accelerate symptom onset in a mouse model of Huntington's disease. PLoS Curr. 2, RRN1201.

Ransome, M. I., 2012. Androgen function in the pathophysiology and treatment of male Huntington's disease patients. J Neuroendocrinol.

Ransome, M. I. & Turnley, A. M., 2007. Systemically delivered Erythropoietin transiently enhances adult hippocampal neurogenesis. J Neurochem. 102, 1953-65.

Ransome, M. I. & Turnley, A. M., 2008. Growth hormone signaling and hippocampal neurogenesis: insights from genetic models. Hippocampus. 18, 1034-50.

Ransome, M. I., Renoir, T., &Hannan, A. J., 2012. Hippocampal Neurogenesis, Cognitive Deficits and Affective Disorder in Huntington's Disease. Neural Plast. 2012, 874387.

Reiner, A., et al., 1988. Differential loss of striatal projection neurons in Huntington disease. Proc Natl Acad Sci U S A. 85, 5733-7.

Rotwein, P., 2012. Mapping the growth hormone--Stat5b--IGF-I transcriptional circuit. Trends Endocrinol Metab. 23, 186-93.

Sapp, E., et al., 2001. Early and progressive accumulation of reactive microglia in the Huntington disease brain. J Neuropathol Exp Neurol. 60, 161-72.

Sasaki, Y., et al., 2001. Iba1 is an actin-cross-linking protein in macrophages/microglia. Biochem Biophys Res Commun. 286, 292-7.

Scholzen, T. & Gerdes, J., 2000. The Ki-67 protein: from the known and the unknown. J Cell Physiol. 182, 311-22.

Silver, J. & Miller, J. H., 2004. Regeneration beyond the glial scar. Nat Rev Neurosci. 5, 146-56.

Simpson, J. M., et al., 2011. Altered adult hippocampal neurogenesis in the YAC128 transgenic mouse model of Huntington disease. Neurobiol Dis. 41, 249-60.

Tai, Y. F., et al., 2007. Microglial activation in presymptomatic Huntington's disease gene carriers. Brain. 130, 1759-66.

Tashiro, A., Makino, H., &Gage, F. H., 2007. Experience-specific functional modification of the dentate gyrus through adult neurogenesis: a critical period during an immature stage. J Neurosci. 27, 3252-9.

Trejo, J. L., Carro, E., &Torres-Aleman, I., 2001. Circulating insulin-like growth factor I mediates exercise-induced increases in the number of new neurons in the adult hippocampus. J Neurosci. 21, 1628-34.

Trejo, J. L., Llorens-Martin, M. V., &Torres-Aleman, I., 2007. The effects of exercise on spatial learning and anxiety-like behavior are mediated by an IGF-I-dependent mechanism related to hippocampal neurogenesis. Mol Cell Neurosci.

Trembath, M. K., et al., 2010. A retrospective study of the impact of lifestyle on age at onset of Huntington disease. Mov Disord. 25, 1444-50.

van Praag, H., Kempermann, G., &Gage, F. H., 1999a. Running increases cell proliferation and neurogenesis in the adult mouse dentate gyrus. Nat Neurosci. 2, 266-70.

van Praag, H., et al., 1999b. Running enhances neurogenesis, learning, and long-term potentiation in mice. Proc Natl Acad Sci U S A. 96, 13427-31.

Vandenbosch, R., et al., 2009. Adult neurogenesis and the diseased brain. Curr Med Chem. 16, 652-66.

Wachs, F. P., et al., 2006. Transforming growth factor-beta1 is a negative modulator of adult neurogenesis. J Neuropathol Exp Neurol. 65, 358-70.

Wellington, C. L., et al., 1998. Caspase cleavage of gene products associated with triplet expansion disorders generates truncated fragments containing the polyglutamine tract. J Biol Chem. 273, 9158-67.

Williams, C. A. & Lavik, E. B., 2009. Engineering the CNS stem cell microenvironment. Regen Med. 4, 865-77.

Zajac, M. S., et al., 2010. Wheel running and environmental enrichment differentially modify exon-specific BDNF expression in the hippocampus of wild-type and pre-motor symptomatic male and female Huntington's disease mice. Hippocampus. 20, 621-36.

Figure legends:

Figure 1. Schematic representing designs for experiment#1 (A), experiment#2 (B) and experiment#3 (C). IHC, immunohistochemistry.

Figure 2. Voluntary running activity was analyzed in wildtype (WT) and R6/1 HD female and male mice. Individually housed mice with running wheels and had their distances monitored daily and recorded in meters run per 24 hours. Female WT mice consistently engaged in more voluntary running compared to female HD mice (A). This observation was also observed in male WT mice compared to HD males (B). Two-way ANOVA showed that female mice undertake more voluntary running activity compared to males within both genotypes and demonstrated the stark reduction in running distances in male HD mice (C). *P<0.05, **P<0.01, ***P<0.001, 2-way ANOVA, Bonferroni's pair-wise test.

Figure 3. Proliferation of sub-granular zone (SGZ) precursor cells was examined in wildtype and R6/1 HD female and male mice under standard housing conditions (control) and in response to voluntary running (run) using 3-way ANOVA (genotype x sex x housing). The volume of the sampled SGZ was unchanged regardless of sex, genotype or housing condition (A). Voluntary running robustly increased Ki67(+) cell density in female and male wildtype mice compared to genotype control housed mice, which was not observed in female or male R6/1 HD mice (B). The density of BrdU(+) cells was increased in running female and male wildtype mice compared to control-housed sex-matched wildtypes, which again was not observed in female or male R6/1 HD mice (C). Multiple pair-wise comparisons were made using the Least Significant Difference test and are detailed for both Ki67 and BrdU-positive cell densities in table 1 and described in full in the results. Images in (B) and (C) are representative of Ki67 and BrdU immunohistochemistry, respectively, with the defined SGZ demarcated by dashed lines (see methods section) and scar bars=50μm.

Figure 4. Early neuronal differentiation of sub-granular zone precursor cells was examined in wildtype and R6/1 HD female and male mice under standard housing conditions (control) and in response to voluntary running (run) using 3-way ANOVA (genotype x sex x housing). Double-

label immunofluorescence combining doublecortin (DCX, red) and BrdU (green) was imaged by confocal microscopy and reconstructed in 3-dimensions to analyze BrdU/DCX co-labeling (A). Housing had a significant main effect on the proportion of BrdU(+) cells co-labeling with DCX (B). Table 2 details P-values obtained from multiple pair-wise comparisons made using the Least Significant Difference test, which are described in full in the results. Scale bar=50μm.

Figure 5. Quantitative analysis of **c-Fos expression in surviving mature adult-generated hippocampal neurons** was performed in female wildtype and R6/1 HD mice in standard housing (control) and enriched housing (run+enrich) using 2-way ANOVA (genotype x housing). BrdU immunohistochemistry was employed to quantify cell survival in the sub-granular zone (SGZ)/granule cell layer (GCL) 42 days after final intraperitoneal BrdU injections (A). No change in the volume of the sampled GCL was observed between any of groups (B). Analysing BrdU(+) cell density showed that sequential running followed by enrichment stimulated a 3-fold increase in surviving cells in wildtype animals and while base-line cell survival in R6/1 HD mice was doubled the deficits were not fully rescued (C). Triple-label immunofluorescence combining c-Fos (green), BrdU (red) and NeuN (blue) were imaged by confocal microscopy and reconstructed in 3-dimensions to analyze BrdU/NeuN/c-Fos co-labeling with a representative image shown in (D), where panel 'a' shows NeuN and c-Fos (blue and green channels), 'b' shows NeuN and BrdU (blue and red channels) and 'c' shows a full 3-dimensional reconstruction of a triple-labeled cell in a R6/1 HD mouse. Neural differentiation (BrdU/NeuN co-labeling) was unchanged by genotype or housing (E). Expression of the immediate early gene c-Fos (green) was used in conjunction with NeuN (blue) and BrdU (red) as an indirect measure of **neuronal activation** (see methods and results sections). Triple-label analysis demonstrated very low **proportions of c-Fos/BrdU/NeuN co-labeling** that were unchanged between any of the experimental groups (F). *P<0.05, **P<0.01, two-way ANOVA. Scale bar = 50μm in A (all panels) and 20μm in D (all panels).

Figure 6. Components of Insulin-like growth factor-1 (IGF-1) signaling were analyzed in wildtype and R6/1 HD female mice. ELISA measurements of growth hormone (GH) (A) and IGF-1 (B) concentrations were performed on serum derived from mice in control housing during the day, control housing during the night and after 2 hours of running during the night using 2-

way ANOVA (genotype x housing). Acute running increased serum GH concentrations in both genotypes, while no change between wildtype and R6/1 HD female mice was observed. Acute running also increased serum IGF-1 concentrations in wildtype female mice compared to their day-time controls, during which the female R6/1 HD mice had higher concentration compared to female wildtypes. Western blot analysis of Akt-signaling was performed on whole hippocampal tissue derived from female wildtype and R6/1 HD mice in standard housing (control) and after 8 days of voluntary running (run) and analyzed by 2-way ANOVA (genotype x housing). Quantitative analysis showed no change in IGF-1 receptor (IGF-1R) protein levels (C). Running increased phosphorylation levels of Akt at serine(473) in female wildtypes but not R6/1 HD mice and basal levels of total Akt protein were decreased in control and running female R6/1 HD mice compared to wildtypes (D). Quantitative immunohistochemistry in wildtype and R6/1 HD female mice under standard housing conditions (control) and in response to voluntary running (run) showed no change in the density of activated caspase-3(+) cells in the sub-granular zone(SGZ)/granule cell layer (GCL) (E). **P*<0.05, **P*<0.01, two-way ANOVA with Bonferroni's pair-wise test. Scale bar=50μm in (E).

Figure 7. Concentrations of transforming growth factor-β (TGFβ) were measured by ELISA in serum derived from female wildtype and R6/1 HD mice in control housing during the day, control housing during the night and after 2 hours of running during the night and analyzed using 2-way ANOVA (genotype x housing). TGFβ serum concentrations were increased in night wildtype female mice compared to running female wildtypes (A). Double-label immunofluorescence combining Iba-1 (green) and BrdU (red) was imaged by confocal microscopy and reconstructed in 3-dimensions to quantify BrdU/Iba-1 co-labeling showing no change between female wildtype and R6/1 HD standard housed mice (B). Immunohistochemistry was used to identify Iba-1(+) microglia in granule cell layer (GCL), sub-granular zone (SGZ) and hilus regions of the hippocampus in wildtype and R6/1 HD mice (C). The density of Iba-1(+) cells in the GCL of R6/1 HD mice was decreased compared to wildtypes, while no change was observed in the SGZ or hilus regions (C). Quantifying total Iba-1 protein levels by Western blot showed comparative levels in the hippocampi of standard-housed female wildtype and R6/1 HD mice (D). Western blot quantitation of hippocampal glial fibrillary acid protein (GFAP) levels were not changed in standard housed female R6/1 HD mice compared to wildtypes (E). **P*<0.05,

student's *T*-test; ***P*<0.01, two-way ANOVA with Bonferroni's pair-wise test. Scale Bar = 25μm in B; 50μm in A (both panels).

Figure 8. High resolution three-dimensional reconstruction of fluorescent confocal images in 1μm steps through the entire z-axis were used to analyze protein aggregates containing mutant Huntingtin (mHtt). Dense mHtt immunoreactivity (red in A, B, C, D, F and G; green in E) was observed in the granule cell layer (GCL) of female R6/1 HD mice but not found in proliferating cells (Ki67, green, A) or newly-generated cells from 1 to 7 days old (BrdU, green, B) in the sub granular zone (SGZ). Adult-generated cells up to 42 days old (BrdU, green, C) were found in close proximity to mHtt aggregates but were never observed to fully co-label. The dashed box 'a' is shown enlarged and reconstructed with the red signal designating mHtt evident between 4 and 6μm of the z-axis and the green signal designating a BrdU-labeled cell evident between 7 and 11μm of the z-axis and a full z-axis reconstruction with orthogonal views demonstrating the close proximity but incomplete overlap of the red and green signals. A similar enlarged reconstruction is also shown for the BrdU(+) cell bound by the dashed box 'b'. In contrast, nearly 60% of the c-Fos(+) cells in the GCL (green, D) showed co-labeling with discrete mHtt immunoreactivity as demonstrated by the enlarged reconstruction of the c-Fos(+) cell bounded by dashed box 'a', where the red signal designating mHtt is evident between 7 and 9μm of the z-axis and the green signal designating a c-Fos(+) cell evident between 1 and 9μm of the z-axis and a full z-axis reconstruction with orthogonal views demonstrating the red and green signal overlap. A similar enlarged reconstruction is shown for the c-Fos(+) cell bound by the dashed box 'b', demonstrating an example of the 40% of c-Fos(+) cells showing no overlap between red and green signals. Non-neural cells populating the hippocampal neurogenic niche were also examined with lectin(+) endothelium (red, E), glial fibrillary acidic protein (GFAP)(+) astrocytes (green, F) and Iba-1(+) microglia (green, G) not demonstrating any co-labeling with mHtt. Scale bars = 20μm in all panels. The dashed white lines in A, B, E, F and G represent the SGZ, while the 2 dashed white lines in the main panels of C and D demarcate the GCL.

Table 1. *P* values of 3-way ANOVA LSD pair-wise comparisons for Ki67$^{(+)}$ and BrdU$^{(+)}$ cell densities (Fig. 2).

BrdU \ **Ki67**	WT ♀ Con	**HD** ♀ Con	WT ♀ Run	**HD** ♀ Run	WT ♂ Con	**HD** ♂ Con	WT ♂ Run	**HD** ♂ Run
WT ♀ Con		ns	<.001	ns	ns	ns	<.001	ns
HD ♀ Con	**<0.01**		<.001	ns*	ns	ns	<.001	ns
WT ♀ Run	<.001	<.001		<.001	<.001	<.001	ns	<.001
HD ♀ Run	ns	ns*	<.001		ns	<.05	<.005	<.05
WT ♂ Con	ns	ns	<.001	ns		<.05	<.001	<.05
HD ♂ Con	**<.01**	ns	<.001	<.05	<.05		<.001	ns
WT ♂ Run	**ns**	<.001	**<.001**	<.005	<.05	<.001		<.001
HD ♂ Run	**<.01**	ns	<.001	<.05	<.05	ns	<.001	

HD ♂ Run	**<.05**	ns	<.001	**ns**	**ns**	ns

<.001

WT, wildtype; HD, R6/1 Huntington's disease; Con, standard-housed control; Run, running-wheel housed;

♀, female; ♂ male.

Table 2. *P* values of 3-way ANOVA LSD pair-wise comparisons for BrdU/DCX co-labeling (Fig. 3).

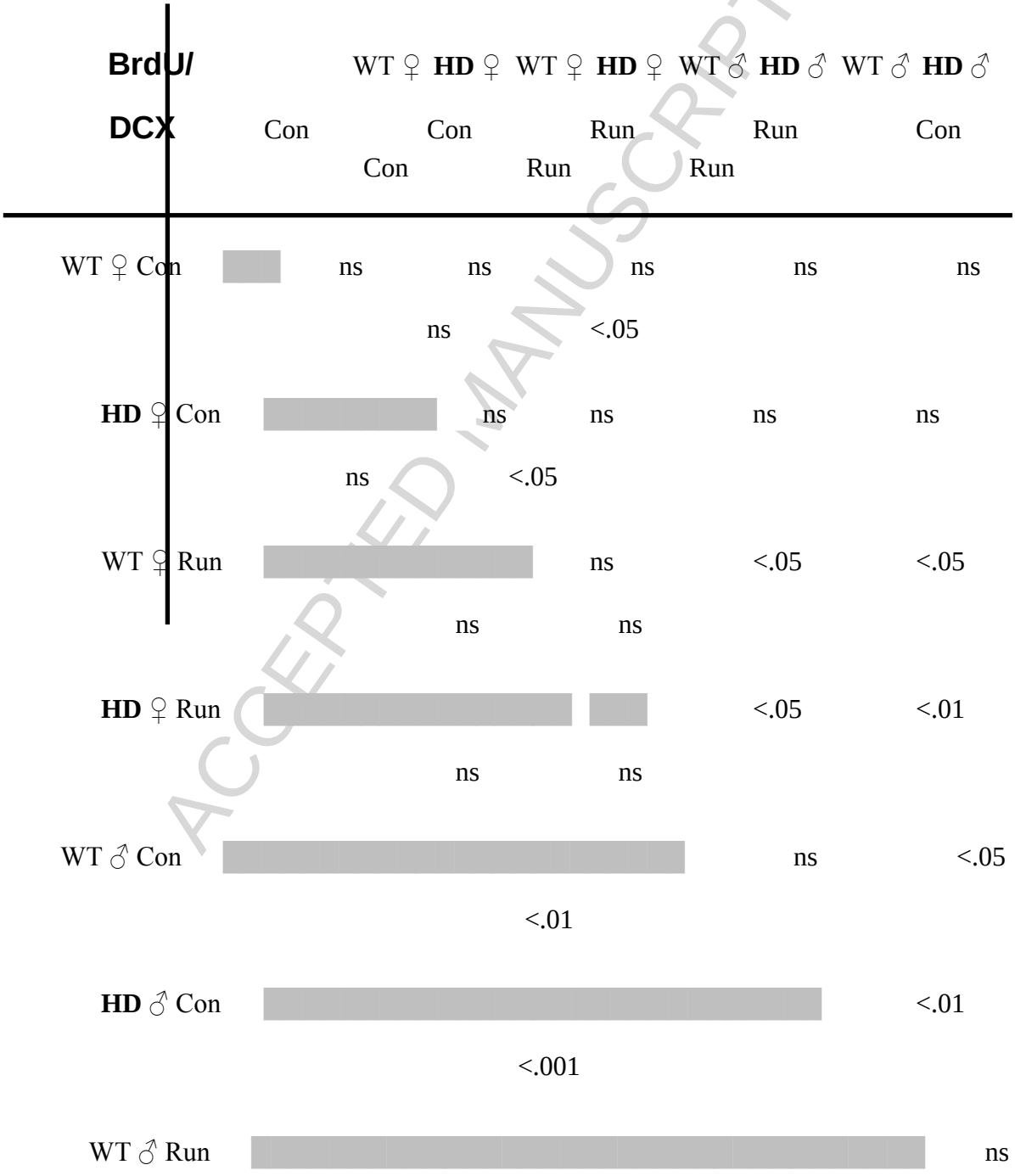

HD ♂ Run

WT, wildtype; HD, R6/1 Huntington's disease; Con, standard-housed control; Run, running-wheel housed;

♀, female; ♂ male.

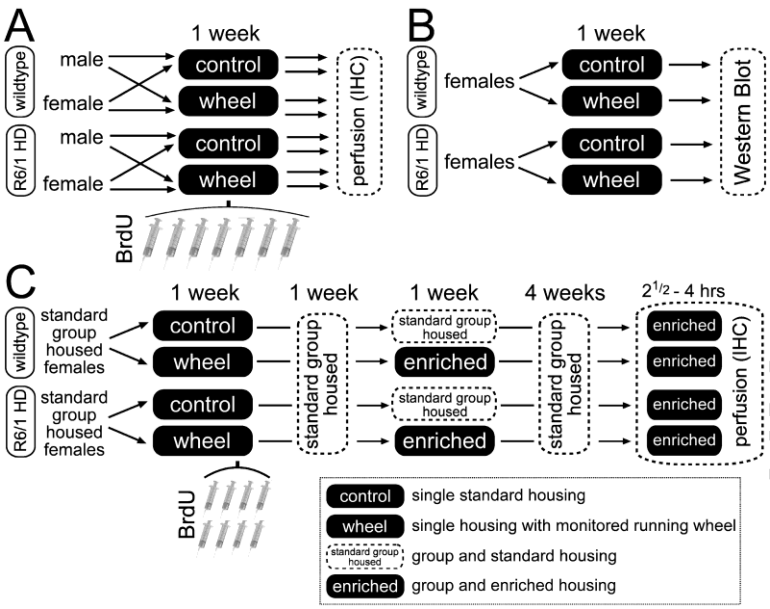

Figure 1

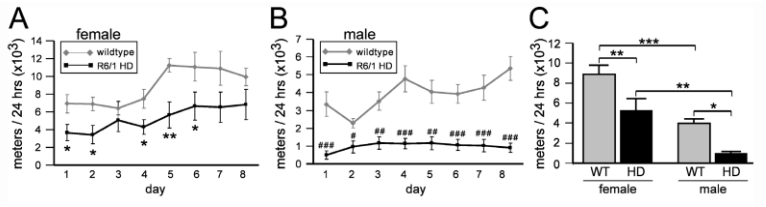

Figure 2

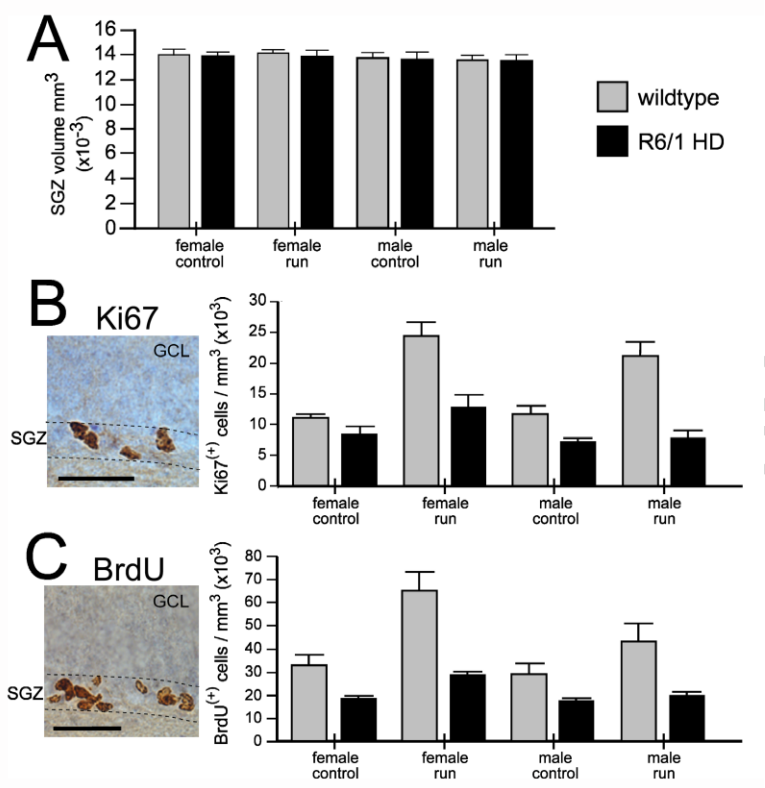

Figure 3

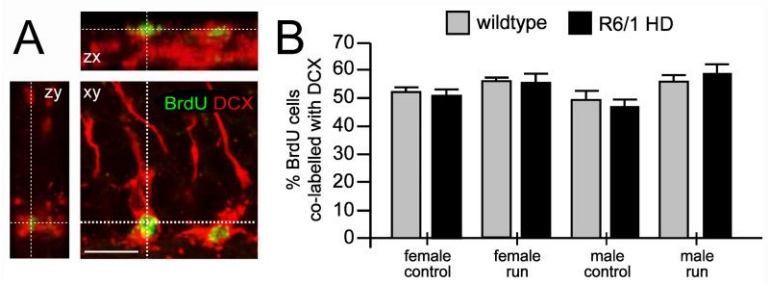

Figure 4

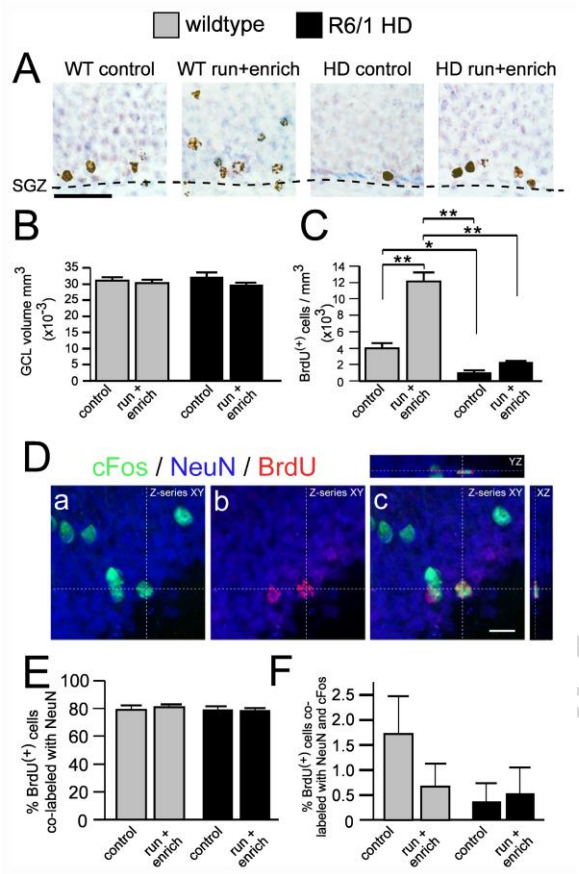

Figure 5

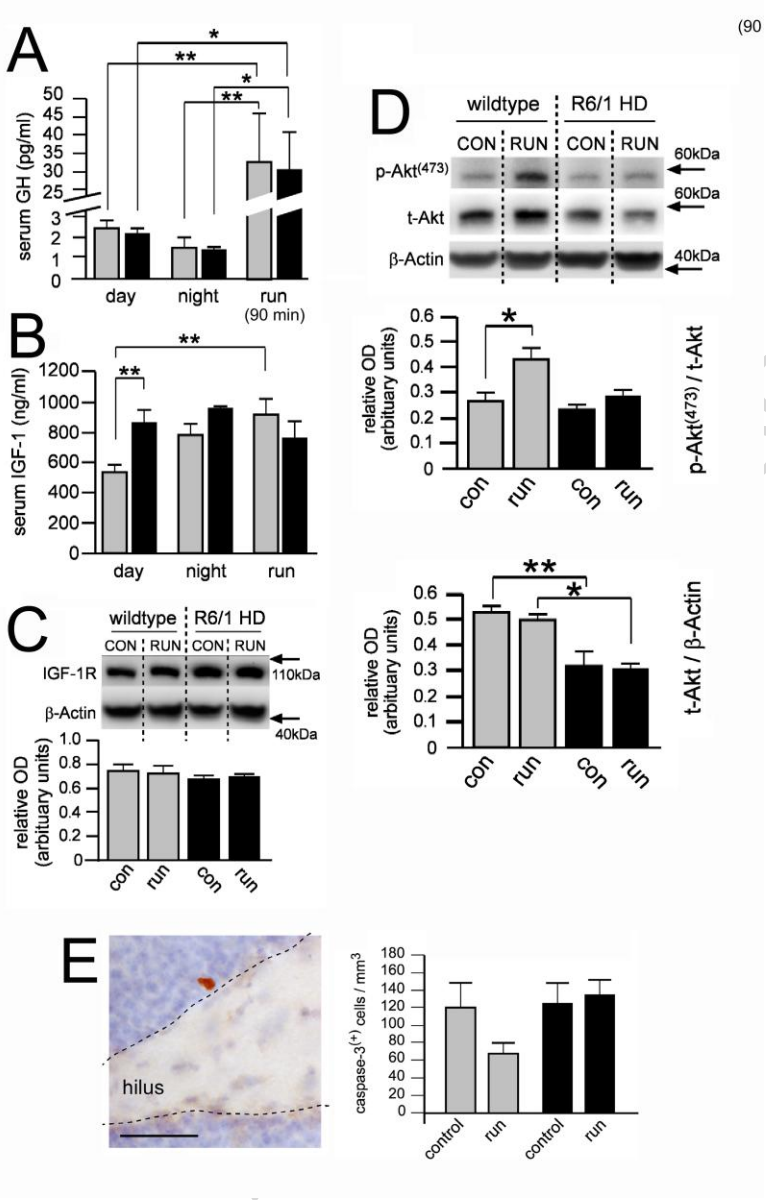

Figure 6

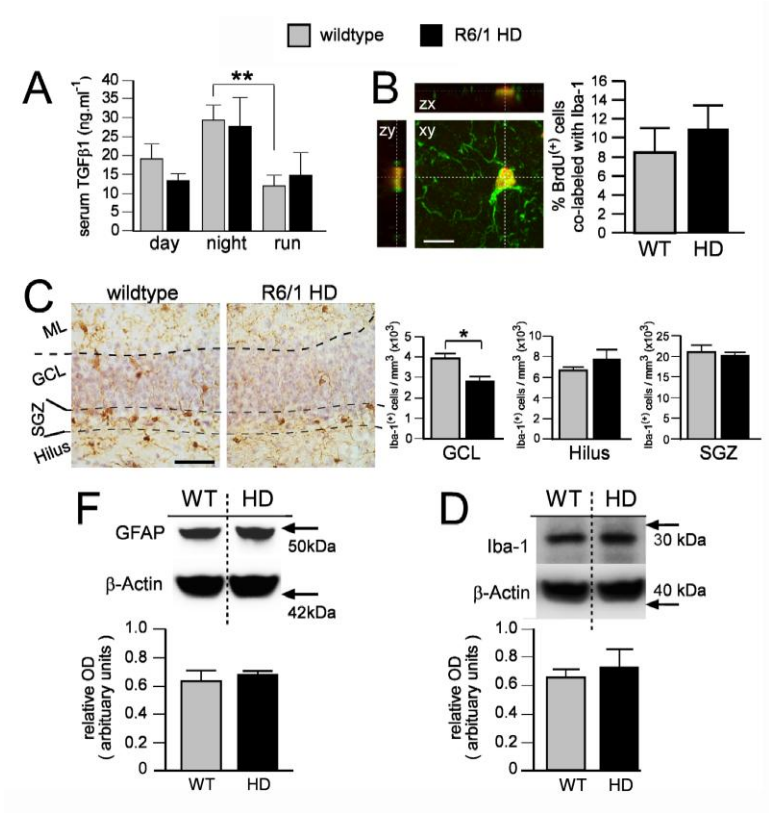

Figure 7

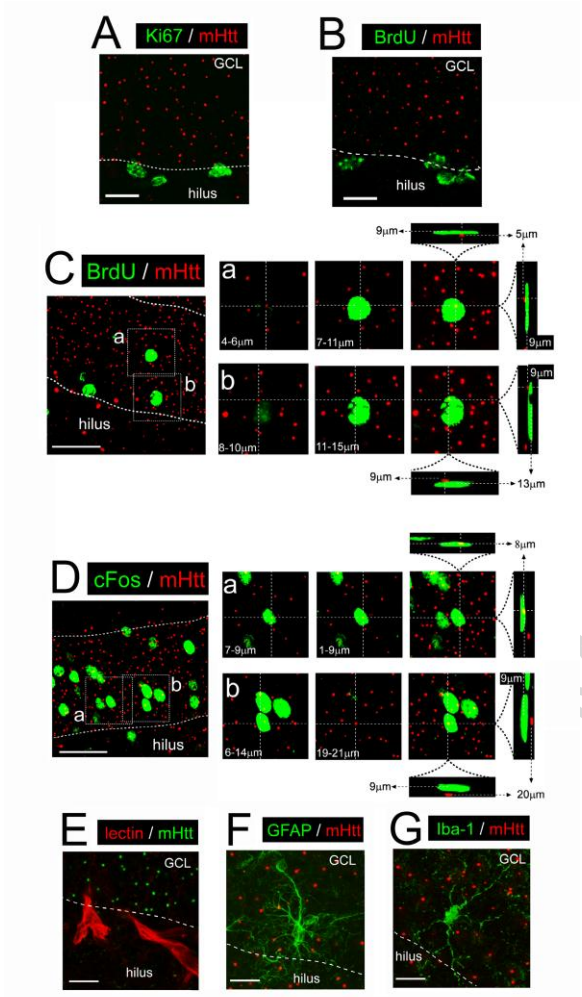

Figure 8

Author/s:
Ransome, MI; Hannan, AJ

Title:
Impaired basal and running-induced hippocampal neurogenesis coincides with reduced Akt signaling in adult R6/1 HD mice

Date:
2013-05-01

Citation:
Ransome, M. I. & Hannan, A. J. (2013). Impaired basal and running-induced hippocampal neurogenesis coincides with reduced Akt signaling in adult R6/1 HD mice. MOLECULAR AND CELLULAR NEUROSCIENCE, 54, pp.93-107. https://doi.org/10.1016/j.mcn.2013.01.005.